PHYSICAL REVIEW D **89,** 074031 (2014)

Direct *CP* asymmetries of three-body *B* decays in perturbative QCD

Wen-Fei Wang,[1,*] Hao-Chung Hu,[2,3,†] Hsiang-nan Li,[3,4,5,‡] and Cai-Dian Lü[1,§]

[1]*Institute of High Energy Physics and Theoretical Physics Center for Science Facilities, Chinese Academy of Sciences, Beijing 100049, People's Republic of China*
[2]*Department of Physics, National Taiwan University, Taipei, Taiwan 106, Republic of China*
[3]*Institute of Physics, Academia Sinica, Taipei, Taiwan 115, Republic of China*
[4]*Department of Physics, National Tsing-Hua University, Hsinchu, Taiwan 300, Republic of China*
[5]*Department of Physics, National Cheng-Kung University, Tainan, Taiwan 701, Republic of China*

(Received 1 March 2014; published 11 April 2014)

We propose a theoretical framework for analyzing three-body hadronic B meson decays based on the perturbative QCD approach. The crucial nonperturbative input is a two-hadron distribution amplitude for final states, whose timelike form factor and rescattering phase are fit to relevant experimental data. Together with the short-distance strong phase from the b-quark decay kernel, we are able to make predictions for direct CP asymmetries in, for example, the $B^\pm \to \pi^+\pi^-\pi^\pm$ and $\pi^+\pi^-K^\pm$ modes, which are consistent with the LHCb data in various localized regions of phase space. Applications of our formalism to other three-body hadronic and radiative B meson decays are mentioned.

DOI: 10.1103/PhysRevD.89.074031 PACS numbers: 13.20.He, 13.25.Hw, 13.30.Eg

Three-body hadronic B meson decays have been studied for many years [1–4]. They attracted much attention recently, after the LHCb Collaboration measured sizable direct CP asymmetries in localized regions of phase space [5–7], such as

$$A_{CP}^{\rm reg}(\pi^+\pi^-\pi^+) = 0.584 \pm 0.082 \pm 0.027 \pm 0.007, \quad (1)$$

for $m^2_{\pi^+\pi^-{\rm high}} > 15\ {\rm GeV}^2$ and $m^2_{\pi^+\pi^-{\rm low}} < 0.4\ {\rm GeV}^2$, and

$$A_{CP}^{\rm reg}(\pi^+\pi^-K^+) = 0.678 \pm 0.078 \pm 0.032 \pm 0.007, \quad (2)$$

for $m^2_{K^+\pi^-{\rm high}} < 15\,{\rm GeV}^2$ and $0.08 < m^2_{\pi^+\pi^-{\rm low}} < 0.66\,{\rm GeV}^2$. Theoretical attempts to understand these data were made: The above CP asymmetries were attributed to the interference between a light scalar and intermediate resonances in [8]; the relations among the above CP asymmetries in the U-spin symmetry limit were examined in [9]; SU(3) and U-spin symmetry breaking effects were included in the amplitude parametrization in [10]; in [11] the nonresonant contributions were parametrized in the framework of heavy meson chiral perturbation theory [12]; and the resonant contributions were estimated by means of the usual Breit-Wigner formalism.

Viewing the experimental progress, it is important to construct a corresponding framework based on the factorization theorem, in which perturbative evaluation can be performed systematically with controllable nonperturbative inputs. Motivated by its theoretical self-consistency and phenomenological success, we shall generalize the perturbative QCD (PQCD) approach [13,14] to three-body hadronic B meson decays. A direct evaluation of hard b-quark decay kernels, which contain two virtual gluons at leading order (LO), is not practical because of the enormous number of diagrams. Besides, the contribution from two hard gluons is power suppressed and is not important. In this region all three final-state mesons carry momenta of $O(m_B)$, and all three pairs of them have invariant masses of $O(m_B^2)$, m_B being the B meson mass. The dominant contribution comes from the region where at least one pair of light mesons has an invariant mass below $O(\bar\Lambda m_B)$ [1], $\bar\Lambda = m_B - m_b$ being the B meson and b quark mass difference. The configuration involves two energetic mesons almost collimating to each other, in which the dynamics associated with the pair of mesons can be factorized into a two-meson distribution amplitude $\phi_{h_1h_2}$ [15]. It is evident that $\phi_{h_1h_2}$ appropriately describes the nonperturbative dynamics of a two-meson system in the localized region of phase space, say, $m^2_{\pi^+\pi^-{\rm low}} < 0.4\ {\rm GeV}^2$.

With the introduction of a two-meson distribution amplitude, the LO diagrams for three-body hadronic B meson decays reduce to those for two-body decays, as displayed in Figs. 1–4. The PQCD factorization formula for a $B \to h_1h_2h_3$ decay amplitude is then written as [1]

$$\mathcal{A} = \phi_B \otimes H \otimes \phi_{h_1h_2} \otimes \phi_{h_3}, \quad (3)$$

where the hard kernel H contains only a single hard gluon. The B meson (h_1-h_2 pair, h_3 meson) distribution amplitude ϕ_B ($\phi_{h_1h_2}$, ϕ_{h_3}) absorbs nonperturbative dynamics characterized by the soft scale $\bar\Lambda$ (the invariant mass of the meson pair, the h_3 meson mass). Figure 1 involves the transition of the B meson into two light mesons. The amplitude from

*wangwf@ihep.ac.cn
†hchu@phys.sinica.edu.tw
‡hnli@phys.sinica.edu.tw
§lucd@ihep.ac.cn

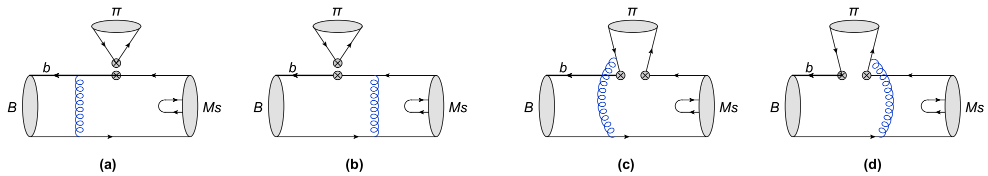

FIG. 1 (color online). Single-pion emission diagrams for the $B^+ \to \pi^+\pi^-\pi^+$ decay, where Ms stands for the pion pair.

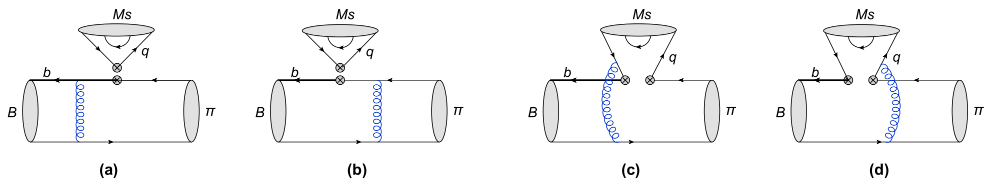

FIG. 2 (color online). Two-pion emission diagrams, where q denotes a u or d quark.

Fig. 2 is expressed as a product of a heavy-to-light form factor and a timelike light-light form factor in the heavy-quark limit. In Figs. 3 and 4, a B meson annihilates completely, and three light mesons are produced.

Take Fig. 1(a) for the $B^+ \to \pi^+\pi^-\pi^+$ decay as an example, in which the B^+ meson momentum p_B, the total momentum $p = p_1 + p_2$ of the pion pair, and the momentum p_3 of the second π^+ meson are chosen, in light-cone coordinates, as

$$p_B = \frac{m_B}{\sqrt{2}}(1, 1, 0_{\rm T}), \qquad p = \frac{m_B}{\sqrt{2}}(1, \eta, 0_{\rm T}),$$
$$p_3 = \frac{m_B}{\sqrt{2}}(0, 1-\eta, 0_{\rm T}), \tag{4}$$

with the variable $\eta = \omega^2/m_B^2$, $\omega^2 = p^2$ being the invariant mass squared. The momenta p_1 and p_2 of the π^+ and π^- mesons in the pair, respectively, have the components

$$p_1^+ = \zeta\frac{m_B}{\sqrt{2}}, \qquad p_1^- = (1-\zeta)\eta\frac{m_B}{\sqrt{2}}, \qquad p_2^+ = (1-\zeta)\frac{m_B}{\sqrt{2}},$$
$$p_2^- = \zeta\eta\frac{m_B}{\sqrt{2}}, \tag{5}$$

with the π^+ meson momentum fraction ζ. The momenta of the spectators in the B meson, the pion pair, and the π^+ meson read, respectively, as

$$k_B = \left(0, \frac{m_B}{\sqrt{2}}x_B, k_{B\rm T}\right), \qquad k = \left(\frac{m_B}{\sqrt{2}}z, 0, k_{\rm T}\right),$$
$$k_3 = \left(0, \frac{m_B}{\sqrt{2}}(1-\eta)x_3, k_{3\rm T}\right). \tag{6}$$

The definitions of the two-pion distribution amplitudes in terms of hadronic matrix elements of nonlocal quark operators up to twist 3 can be found in [1,15,16]. We parametrize them at the leading partial waves as

$$\phi_{\pi\pi}^{v,t}(z, \zeta, \omega^2) = \frac{3F_{\pi,t}(\omega^2)}{\sqrt{2N_c}}z(1-z)(2\zeta-1), \tag{7}$$

$$\phi_{\pi\pi}^{s}(z, \zeta, \omega^2) = \frac{3F_{s}(\omega^2)}{\sqrt{2N_c}}z(1-z), \tag{8}$$

with the number of colors N_c, where the factor $2\zeta - 1$ arises from the Legendre polynomial $P_l(2\zeta - 1)$ for $l = 1$.

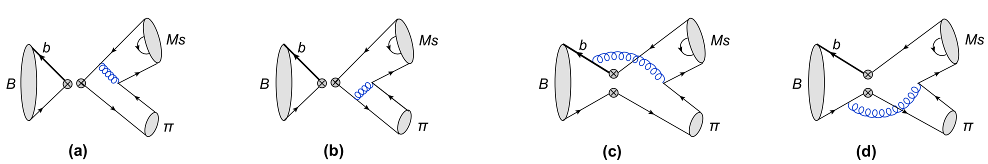

FIG. 3 (color online). Annihilation diagrams.

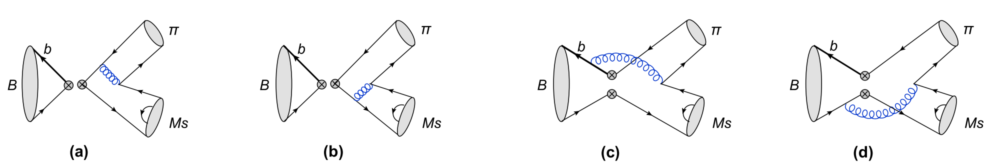

FIG. 4 (color online). More annihilation diagrams.

The PQCD power counting indicates the scaling of the vector-current form factor in the asymptotic region, $F_\pi(w^2) \sim 1/w^2$, and the relative importance of the scalar-current and tensor-current form factors, $F_{s,t}(w^2)/F_\pi(w^2) \sim m_0^\pi/w$, where $m_0^\pi = m_\pi^2/(m_u + m_d)$ is the chiral scale associated with the pion, with m_π, m_u, and m_d being the masses of the pion, the u quark, and the d quark, respectively. To evaluate the nonresonant contribution in the arbitrary range of w^2, we propose the parametrization for the complex timelike form factors

$$F_\pi(w^2) = \frac{m^2 \exp[i\delta_1^1(w)]}{w^2 + m^2}, \qquad F_t(w^2) = \frac{m_0^\pi m^2 \exp[i\delta_1^1(w)]}{w^3 + m_0^\pi m^2},$$
$$F_s(w^2) = \frac{m_0^\pi m^2 \exp[i\delta_0^0(w)]}{w^3 + m_0^\pi m^2}, \tag{9}$$

in which the parameter $m = 1$ GeV is determined by the fit to the experimental data $m_{J/\psi}^2 |F_\pi(m_{J/\psi}^2)|^2 \sim 0.9\ \mathrm{GeV}^2$ [17], $m_{J/\psi}$ being the J/ψ meson mass. The resultant w^2 dependence of $F_\pi(w^2)$ also agrees with the low-energy data of the timelike pion electromagnetic form factor for $w < 1$ GeV [18], and with the next-to-leading-order (NLO) PQCD calculation [19]. The strong phases δ_l^I are chosen as the phase shifts for the S wave ($I = 0$, $l = 0$) and P wave ($I = 1$, $l = 1$) of elastic $\pi\pi$ scattering [16] according to Watson's theorem. We simply parametrize the data of these strong phases [20–22] for $2m_\pi < w < 0.7$ GeV as

$$\delta_0^0(w) = \pi(w - 2m_\pi), \qquad \delta_1^1(w) = 1.4\pi(w - 2m_\pi)^2, \tag{10}$$

in which $2m_\pi$ represents the $\pi\pi$ threshold. The increase of δ_1^1 with w in the above expression is consistent with the NLO PQCD result of the timelike pion electromagnetic form factor [19].

The B meson, pion, and kaon distribution amplitudes are the same as those widely adopted in the PQCD approach to two-body hadronic B meson decays. We have the B meson distribution amplitude

$$\phi_B(x,b) = N_B x^2(1-x)^2 \exp\left[-\frac{1}{2}\left(\frac{x m_B}{\omega_B}\right)^2 - \frac{\omega_B^2 b^2}{2}\right], \tag{11}$$

with the shape parameter $\omega_B = 0.45 \pm 0.05$ GeV, and the normalization constant $N_B = 73.67$ GeV being related to the B meson decay constant $f_B = 0.21$ GeV via $\lim_{b\to 0}\int dx \phi_B(x,b) = f_B/(2\sqrt{2N_c})$. The pion and kaon distribution amplitudes up to twist 3, $\phi_i^A(x)$ and $\phi_i^{P,T}(x)$ for $i = \pi, K$, are chosen as [23]

$$\phi_i^A(x) = \frac{3f_i}{\sqrt{6}} x(1-x)[1 + a_1 C_1^{3/2}(t) + a_2 C_2^{3/2}(t) + a_4 C_4^{3/2}(t)], \tag{12}$$

$$\phi_i^P(x) = \frac{f_i}{2\sqrt{6}}\left[1 + \left(30\eta_3 - \frac{5}{2}\rho_i^2\right) C_2^{1/2}(t) - 3\left\{\eta_3\omega_3 + \frac{9}{20}\rho_i^2(1 + 6a_2)\right\} C_4^{1/2}(t)\right], \tag{13}$$

$$\phi_i^\sigma(x) = \frac{f_i}{2\sqrt{6}} x(1-x)\left[1 + \left(5\eta_3 - \frac{1}{2}\eta_3\omega_3 - \frac{7}{20}\rho_i^2 - \frac{3}{5}\rho_i^2 a_2\right) C_2^{3/2}(t)\right], \tag{14}$$

with the pion (kaon) decay constant $f_\pi = 0.13$ ($f_K = 0.16$) GeV, the variable $t = 2x - 1$, the Gegenbauer polynomials

$$C_1^{3/2}(t) = 3t, \qquad C_2^{1/2}(t) = \frac{1}{2}(3t^2 - 1), \qquad C_2^{3/2}(t) = \frac{3}{2}(5t^2 - 1),$$
$$C_4^{1/2}(t) = \frac{1}{8}(3 - 30t^2 + 35t^4), \qquad C_4^{3/2}(t) = \frac{15}{8}(1 - 14t^2 + 21t^4), \tag{15}$$

and the mass ratio $\rho_{\pi(K)} = m_{\pi(K)}/m_0^{\pi(K)}$, where $m_0^K = m_K^2/(m_s + m_d)$ is the chiral scale associated with the kaon, m_K and m_s being the masses of the kaon and the s quark, respectively. The Gegenbauer moments $a^{\pi,K}$ are set to [23]

$$a_1^\pi = 0, \qquad a_1^K = 0.06 \pm 0.03,$$
$$a_2^{\pi,K} = 0.25 \pm 0.15, \qquad a_4^\pi = -0.015,$$
$$\eta_3^{\pi,K} = 0.015, \qquad \omega_3^{\pi,K} = -3. \tag{16}$$

The above set of meson distribution amplitudes corresponds to the $B \to \pi$ transition form factors at maximal recoil $F_+^{B\pi}(0) = F_0^{B\pi}(0) = 0.23$ in LO PQCD, which are consistent with the results derived from other approaches [23,24].

The $B^+ \to \pi^+\pi^-\pi^+$ decay width in the localized region of $m_{\pi^+\pi^-\,\mathrm{min}}^2 < m_{\mathrm{min}}^2 = 0.4\ \mathrm{GeV}^2$ and $m_{\pi^+\pi^-\,\mathrm{max}}^2 > m_{\mathrm{max}}^2 = 15\ \mathrm{GeV}^2$ is written as

$$\Gamma = \frac{G_F^2 m_B}{512\pi^4}\int_{\eta_{\mathrm{min}}}^{\eta_{\mathrm{max}}} d\eta(1-\eta)\int_0^{\zeta_{\mathrm{max}}} d\zeta |\mathcal{A}|^2, \tag{17}$$

with the Fermi constant $G_F = 1.16639^{-5}\ \mathrm{GeV}^{-2}$ and the bounds

$$\eta_{\max} = \frac{m_{\min}^2}{m_B^2}, \qquad \eta_{\min} = \frac{4m_\pi^2}{m_B^2},$$
$$\zeta_{\max} = 1 - \frac{m_{\max}^2}{(1-\eta)m_B^2}, \tag{18}$$

where the upper bound $\zeta_{\max}$ is derived from the invariant mass squared $(p_2+p_3)^2$. The contributions from all the diagrams in Figs. 1–4 to the decay amplitude $\mathcal{A}$ are collected in the Appendix. The corresponding formulas for the $B^+ \to \pi^+\pi^-K^+$ decay can be obtained straightforwardly.

Employing the input parameters $\Lambda_{\bar{M}S}^{(f=4)} = 0.25$ GeV, $m_{\pi^\pm} = 0.1396$ GeV, $m_{K^\pm} = 0.4937$ GeV, $m_{B^\pm} = 5.279$ GeV [17,25], and the Wolfenstein parameters in [17], we derive the direct CP asymmetries in the region of $m^2_{\pi^+\pi^-\mathrm{low}} < 0.4\ \mathrm{GeV}^2$ and $m^2_{\pi^+\pi^-\mathrm{or}K^+\pi^-\mathrm{high}} > 15\ \mathrm{GeV}^2$,

$$A_{\mathrm{CP}}(B^\pm \to \pi^+\pi^-\pi^\pm) = 0.519^{+0.124}_{-0.219}(\omega_B)^{+0.108}_{-0.091}(a_2^\pi)^{+0.027}_{-0.032}(m_0^\pi), \tag{19}$$

$$A_{\mathrm{CP}}(B^\pm \to \pi^+\pi^-K^\pm) = -0.018^{+0.024}_{-0.044}(\omega_B)^{+0.006}_{-0.009}(a_2^\pi \ \&\ a_2^K)^{+0.002}_{-0.003}(m_0^\pi \ \&\ m_0^K). \tag{20}$$

The first and second errors come from the variation of $\omega_B = 0.45 \pm 0.05$ GeV and $a_2^{\pi,K} = 0.25 \pm 0.15$, respectively, and the third errors are induced by $m_0^\pi = 1.4 \pm 0.1$ GeV and $m_0^K = 1.6 \pm 0.1$ GeV. The uncertainties caused by the variation of the Wolfenstein parameters λ, A, ρ, η, and of the Gegenbauer moment $a_1^K = 0.06 \pm 0.03$ are very small and have been neglected. While the decay widths are quadratically proportional to the decay constants f_B, f_π and/or f_K, the CP asymmetries are independent of them.

Obviously, our prediction for $A_{CP}(B^\pm \to \pi^+\pi^-\pi^\pm)$ agrees well with the LHCb data. Since the emission contribution and the imaginary annihilation contribution depend on the B meson distribution amplitude in different ways, the variation of ω_B explores the relevance of the short-distance strong phase from the b-quark decay kernel. The sensitivity of the predicted CP asymmetries to ω_B then implies the importance of this strong phase. As the P-wave rescattering phase associated with the pion electromagnetic form factor decreases by half, the predicted CP asymmetries are also reduced by half. The change of the phases associated with the scalar and tensor form factors does not modify the CP asymmetries much. Therefore, we conclude that the short-distance and long-distance P-wave strong phases are equally crucial for the direct CP asymmetries in the localized region of phase space. The LHCb data in Eq. (2) are dominated by the resonant channel $B^\pm \to \rho^0K^\pm$. It is encouraging that the data confirm the NLO PQCD prediction $A_{CP}(B^\pm \to \rho^0K^\pm) = 0.71^{+0.25}_{-0.35}$ [26]. We have checked that our prediction in Eq. (20) for the localized region of phase space is consistent with the LHCb data in Fig. 2 of [5]. Moreover, we have predicted larger $A_{CP}(B^\pm \to \pi^+\pi^-\pi^\pm) = 0.631$ in the region of $m^2_{\pi^+\pi^-\mathrm{low}} < 0.4\ \mathrm{GeV}^2$ and $m^2_{\pi^+\pi^-\mathrm{high}} > 20.5\ \mathrm{GeV}^2$ for the central values of the input parameters, which also matches the data [6].

In this paper we have proposed a promising formalism for three-body hadronic B meson decays based on the PQCD approach. The calculation is greatly simplified with the introduction of the nonperturbative two-hadron distribution amplitude for final states. The timelike form factors and the rescattering phases involved in the two-pion distribution amplitudes have been fixed by experiments, and the B meson, pion, and kaon distribution amplitudes are the same as in the previous PQCD analysis of two-body hadronic B meson decays. Without any free parameters, our results for $A_{CP}(B^\pm \to \pi^+\pi^-\pi^\pm)$ and $A_{CP}(B^\pm \to \pi^+\pi^-K^\pm)$ accommodate well the recent LHCb data in various localized regions of phase space. It has been observed that the short-distance strong phase from the b-quark decay kernel and the final-state rescattering phase are equally important for explaining the measured direct CP asymmetries. The success indicates that our formalism has potential applications to other three-body hadronic and radiative B meson decays [27], if phase shifts from meson-meson scattering can be derived in nonperturbative methods [28,29].

We thank Wei Wang for helpful discussions. This work was partly supported by the National Science Council of R.O.C. under Grant No. NSC-101-2112-M-001-006-MY3, by the National Center for Theoretical Sciences of R.O.C., and by the National Science Foundation of China under Grants No. 11375208, No. 11228512, and No. 11235005.

APPENDIX: DECAY AMPLITUDES

In this appendix we present the PQCD factorization formulas for the diagrams in Figs. 1–4. The sum of the contributions from Figs. 1(a) and 1(b) gives

$$\mathcal{A}_{1(a,b)} = V_{ub}^* V_{ud} F_{B\to\pi\pi}^{LL} - V_{tb}^* V_{td} (F_{B\to\pi\pi}^{\prime LL} + F_{B\to\pi\pi}^{SP}), \tag{A1}$$

where the amplitudes for the B meson transition into two pions are written as

$$F_{B\to\pi\pi}^{LL} = 8\pi C_F m_B^4 f_\pi \int dx_B dz \int b_B db_B b db \phi_B(x_B, b_B)(1-\eta) \times \{[\sqrt{\eta}(1-2z)(\phi_s+\phi_t) + (1+z)\phi_v] a_1(t_{1a}) E_{1ab}(t_{1a}) h_{1a}(x_B, z, b_B, b) + \sqrt{\eta}(2\phi_s - \sqrt{\eta}\phi_v) a_1(t_{1b}) E_{1ab}(t_{1b}) h_{1b}(x_B, z, b_B, b)\}, \tag{A2}$$

$$F_{B\to\pi\pi}^{\prime LL} = F_{B\to\pi\pi}^{LL}|_{a_1\to a_3}, \tag{A3}$$

$$F_{B\to\pi\pi}^{SP} = -16\pi C_F m_B^4 r f_\pi \int dx_B dz \int b_B db_B b db \phi_B(x_B, b_B) \times \{[\sqrt{\eta}(2+z)\phi_s - \sqrt{\eta} z\phi_t + (1+\eta(1-2z))\phi_v] a_5(t_{1a}) E_{1ab}(t_{1a}) h_{1a}(x_B, z, b_B, b) + [2\sqrt{\eta}(1-x_B+\eta)\phi_s + (x_B-2\eta)\phi_v] a_5(t_{1b}) E_{1ab}(t_{1b}) h_{1b}(x_B, z, b_B, b)\}, \tag{A4}$$

with $r = m_0^\pi/m_B$ and $\phi_{s,t,v} \equiv \phi_{s,t,v}(z, \zeta, \omega^2)$. The Wilson coefficients in the above expressions are defined as $a_1 = C_1/N_c + C_2$, $a_3 = C_3/N_c + C_4 + C_9/N_c + C_{10}$, and $a_5 = C_5/N_c + C_6 + C_7/N_c + C_8$. The spectator diagrams in Figs. 1(c) and 1(d) lead to

$$\mathcal{A}_{1(c,d)} = V_{ub}^* V_{ud} M_{B\to\pi\pi}^{LL} - V_{tb}^* V_{td}(M_{B\to\pi\pi}^{\prime LL} + M_{B\to\pi\pi}^{LR}), \tag{A5}$$

with the amplitudes

$$M_{B\to\pi\pi}^{LL} = 32\pi C_F m_B^4/\sqrt{2N_c} \int dx_B dz dx_3 \int b_B db_B b_3 db_3 \phi_B(x_B, b_B)\phi_\pi^A(1-\eta) \times \{[\sqrt{\eta} z(\phi_s+\phi_t) + ((1-\eta)(1-x_3) - x_B + z\eta)\phi_v] C_1(t_{1c}) E_{1cd}(t_{1c}) h_{1c}(x_B, z, x_3, b_B, b_3) - [z(\sqrt{\eta}(\phi_s-\phi_t)+\phi_v) + (x_3(1-\eta)-x_B)\phi_v] C_1(t_{1d}) E_{1cd}(t_{1d}) h_{1d}(x_B, z, x_3, b_B, b_3)\}, \tag{A6}$$

$$M_{B\to\pi\pi}^{\prime LL} = M_{B\to\pi\pi}^{LL}|_{C_1\to a_9}, \tag{A7}$$

$$M_{B\to\pi\pi}^{LR} = 32\pi C_F r m_B^4/\sqrt{2N_c} \int dx_B dz dx_3 \int b_B db_B b_3 db_3 \phi_B(x_B, b_B) \times \{[\sqrt{\eta} z(\phi_\pi^P+\phi_\pi^T)(\phi_s-\phi_t) + \sqrt{\eta}((1-x_3)(1-\eta)-x_B)(\phi_\pi^P-\phi_\pi^T) \times (\phi_s+\phi_t) - ((1-x_3)(1-\eta)-x_B)(\phi_\pi^P-\phi_\pi^T)\phi_v - \eta z(\phi_\pi^P+\phi_\pi^T)\phi_v] a_7(t_{1c}) E_{1cd}(t_{1c}) h_{1c}(x_B, z, x_3, b_B, b_3) + [\sqrt{\eta} z(\phi_\pi^P-\phi_\pi^T)((\phi_t-\phi_s)+\sqrt{\eta}\phi_v) + (x_B - x_3(1-\eta))(\phi_\pi^P+\phi_\pi^T) \times (\sqrt{\eta}(\phi_s+\phi_t)-\phi_v)] a_7(t_{1d}) E_{1cd}(t_{1d}) h_{1d}(x_B, z, x_3, b_B, b_3)\}, \tag{A8}$$

and the Wilson coefficients $a_7 = C_5 + C_7$ and $a_9 = C_3 + C_9$.

For Figs. 2(a) and 2(b), we have

$$\mathcal{A}_{2(a,b)}^{q=u} = V_{ub}^* V_{ud} F_{B\to\pi}^{LL} - V_{tb}^* V_{td}(F_{B\to\pi}^{\prime LL} + F_{B\to\pi}^{LR}), \tag{A9}$$

$$\mathcal{A}_{2(a,b)}^{q=d} = -V_{tb}^* V_{td}(F_{B\to\pi}^{\prime\prime LL} + F_{B\to\pi}^{\prime LR} + F_{B\to\pi}^{SP}). \tag{A10}$$

The amplitudes involving the $B\to\pi$ transition form factors are expressed as

$$F_{B\to\pi}^{LL} = 8\pi C_F m_B^4 F_\pi(\omega^2) \int dx_B dx_3 \int b_B db_B b_3 db_3 \phi_B(x_B, b_B)(2\zeta-1) \times \{[(1+x_3(1-\eta))(1-\eta)\phi_\pi^A + r(1-2x_3)(1-\eta)\phi_\pi^P + r(1+\eta-2x_3(1-\eta))\phi_\pi^T] \times a_2(t_{2a}) E_{2ab}(t_{2a}) h_{2a}(x_B, x_3, b_B, b_3) + [x_B(1-\eta)\eta\phi_\pi^A + 2r(1-\eta(1+x_B))\phi_\pi^P] a_2(t_{2b}) E_{2ab}(t_{2b}) h_{2b}(x_B, x_3, b_B, b_3)\}, \tag{A11}$$

$$F^{LR}_{B\to\pi} = F^{LL}_{B\to\pi}|_{a_2\to a_6}, \tag{A12}$$

$$F'^{LL}_{B\to\pi} = F^{LL}_{B\to\pi}|_{a_2\to a_4}, \tag{A13}$$

$$F'^{LR}_{B\to\pi} = F^{LL}_{B\to\pi}|_{a_2\to a_8}, \tag{A14}$$

$$F''^{LL}_{B\to\pi} = F^{LL}_{B\to\pi}|_{a_2\to a_{10}}, \tag{A15}$$

$$\begin{aligned} F^{SP}_{B\to\pi} = {} & 16\pi C_F m_B^4\sqrt{\eta}F_\pi(\omega^2)\int dx_B dx_3 \int b_B db_B b_3 db_3 \phi_B(x_B,b_B) \\ & \times\{[(1-\eta)\phi^A_\pi + r(2+x_3(1-\eta))\phi^P_\pi - rx_3(1-\eta)\phi^T_\pi]a'_8(t_{2a})E_{2ab}(t_{2a})h_{2a}(x_B,x_3,b_B,b_3) \\ & + [x_B(1-\eta)\phi^A_\pi + 2r(1-x_B-\eta)\phi^P_\pi]a'_8(t_{2b})E_{2ab}(t_{2b})h_{2b}(x_B,x_3,b_B,b_3)\}, \end{aligned} \tag{A16}$$

in which the Wilson coefficients are given by $a_2 = C_1 + C_2/N_c$, $a_4 = C_3 + C_4/N_c + C_9 + C_{10}/N_c$, $a_6 = C_5 + C_6/N_c + C_7 + C_8/N_c$, $a_8 = C_5 + C_6/N_c - C_7/2 - C_8/(2N_c)$, $a'_8 = C_5/N_c + C_6 - C_7/(2N_c) - C_8/2$, and $a_{10} = [C_3 + C_4 - C_9/2 - C_{10}/2](N_c+1)/N_c$. We derive, from Figs. 2(c) and 2(d),

$$\mathcal{A}^{q=u}_{2(c,d)} = V^*_{ub}V_{ud}M^{LL}_{B\to\pi} - V^*_{tb}V_{td}(M'^{LL}_{B\to\pi} + M^{SP}_{B\to\pi}), \tag{A17}$$

$$\mathcal{A}^{q=d}_{2(c,d)} = -V^*_{tb}V_{td}(M''^{LL}_{B\to\pi} + M^{LR}_{B\to\pi} + M'^{SP}_{B\to\pi}), \tag{A18}$$

with the amplitudes

$$\begin{aligned} M^{LL}_{B\to\pi} = {} & 32\pi C_F m_B^4/\sqrt{2N_c}\int dx_B dz dx_3 \int b_B db_B b db \phi_B(x_B,b_B)\phi_v \\ & \times\{[(1-x_B-z)(1-\eta^2)\phi^A_\pi + rx_3(1-\eta)(\phi^P_\pi - \phi^T_\pi) + r(x_B+z)\eta(\phi^P_\pi + \phi^T_\pi) \\ & - 2r\eta\phi^P_\pi]C_2(t_{2c})E_{2cd}(t_{2c})h_{2c}(x_B,z,x_3,b_B,b) \\ & - [(z-x_B+x_3(1-\eta))(1-\eta)\phi^A_\pi + r(x_B-z)\eta(\phi^P_\pi - \phi^T_\pi) - rx_3(1-\eta)(\phi^P_\pi + \phi^T_\pi)] \\ & \times C_2(t_{2d})E_{2cd}(t_{2d})h_{2d}(x_B,z,x_3,b_B,b)\}, \end{aligned} \tag{A19}$$

$$\begin{aligned} M^{LR}_{B\to\pi} = {} & 32\pi C_F m_B^4\sqrt{\eta}/\sqrt{2N_c}\int dx_B dz dx_3 \int b_B db_B b db \phi_B(x_B,b_B) \\ & \times\{[(1-x_B-z)(1-\eta)(\phi_s+\phi_t)\phi^A_\pi + r(1-x_B-z)(\phi_s+\phi_t)(\phi^P_\pi - \phi^T_\pi) \\ & + r(x_3(1-\eta)+\eta)(\phi_s-\phi_t)(\phi^P_\pi + \phi^T_\pi)]a'_5(t_{2c})E_{2cd}(t_{2c})h_{2c}(x_B,z,x_3,b_B,b) \\ & - [(z-x_B)(1-\eta)(\phi_s-\phi_t)\phi^A_\pi + r(z-x_B)(\phi_s-\phi_t)(\phi^P_\pi - \phi^T_\pi) \\ & + rx_3(1-\eta)(\phi_s+\phi_t)(\phi^P_\pi + \phi^T_\pi)]a'_5(t_{2d})E_{2cd}(t_{2d})h_{2d}(x_B,z,x_3,b_B,b)\}, \end{aligned} \tag{A20}$$

$$\begin{aligned} M^{SP}_{B\to\pi} = {} & 32\pi C_F m_B^4/\sqrt{2N_c}\int dx_B dz dx_3 \int b_B db_B b db \phi_B(x_B,b_B)\phi_v \\ & \times\{[(1+\eta-x_B-z+x_3(1-\eta))(1-\eta)\phi^A_\pi + r\eta(x_B+z)(\phi^P_\pi - \phi^T_\pi) \\ & - rx_3(1-\eta)(\phi^P_\pi + \phi^T_\pi) - 2r\eta\phi^P_\pi]a'_6(t_{2c})E_{2cd}(t_{2c})h_{2c}(x_B,z,x_3,b_B,b) \\ & - [(z-x_B)(1-\eta^2)\phi^A_\pi - rx_3(1-\eta)(\phi^P_\pi - \phi^T_\pi) + r(x_B-z)\eta(\phi^P_\pi + \phi^T_\pi)] \\ & \times a'_6(t_{2d})E_{2cd}(t_{2d})h_{2d}(x_B,z,x_3,b_B,b)\}, \end{aligned} \tag{A21}$$

$$M'^{LL}_{B\to\pi} = M^{LL}_{B\to\pi}|_{C_2\to a'_4}, \tag{A22}$$

$$M''^{LL}_{B\to\pi} = M^{LL}_{B\to\pi}|_{C_2\to a'_{10}}, \tag{A23}$$

$$M'^{SP}_{B\to\pi} = M^{SP}_{B\to\pi}|_{a'_6\to a''_6}, \tag{A24}$$

where the Wilson coefficients are defined as $a'_4 = C_4 + C_{10}$, $a'_5 = C_5 - C_7/2$, $a'_6 = C_6 + C_8$, $a''_6 = C_6 - C_8/2$, and $a'_{10} = C_3 + C_4 - C_9/2 - C_{10}/2$.

The factorizable annihilation diagrams in Figs. 3(a) and 3(b) lead to

$$\mathcal{A}_{3(a,b)} = V^*_{ub}V_{ud}F^{LL}_{a\pi} - V^*_{tb}V_{td}(F'^{LL}_{a\pi} + F^{SP}_{a\pi}), \tag{A25}$$

with the three-pion production amplitudes

$$\begin{aligned} F^{LL}_{a\pi} = {} & 8\pi C_F m_B^4 f_B \int dz dx_3 \int b db b_3 db_3 \\ & \times \{[(x_3(1-\eta)-1)(1-\eta)\phi^A_\pi\phi_v + 2r\sqrt{\eta}(x_3(1-\eta)(\phi^P_\pi - \phi^T_\pi) - 2\phi^P_\pi)\phi_s]a_1(t_{3a})E_{3ab}(t_{3a})h_{3a}(z,x_3,b,b_3) \\ & + [z(1-\eta)\phi^A_\pi\phi_v + 2r\sqrt{\eta}\phi^P_\pi((1-\eta)(\phi_s-\phi_t) + z(\phi_s+\phi_t))]a_1(t_{3b})E_{3ab}(t_{3b})h_{3b}(z,x_3,b,b_3)\}, \end{aligned} \tag{A26}$$

$$F'^{LL}_{a\pi} = F^{LL}_{a\pi}|_{a_1\to a_3}, \tag{A27}$$

$$\begin{aligned} F^{SP}_{a\pi} = {} & 16\pi C_F m_B^4 f_B \int dz dx_3 \int b db b_3 db_3 \\ & \times \{[2\sqrt{\eta}(1-\eta)\phi^A_\pi\phi_s + r(1-x_3)(\phi^P_\pi + \phi^T_\pi)\phi_v + r\eta((1+x_3)\phi^P_\pi - (1-x_3)\phi^T_\pi)\phi_v]a_5(t_{3a})E_{3ab}(t_{3a})h_{3a}(z,x_3,b,b_3) \\ & + [2r(1-\eta)\phi^P_\pi\phi_v + z\sqrt{\eta}((1-\eta)\phi^A_\pi(\phi_s-\phi_t) + 2r\sqrt{\eta}\phi^P_\pi\phi_v)]a_5(t_{3b})E_{3ab}(t_{3b})h_{3b}(z,x_3,b,b_3)\}. \end{aligned} \tag{A28}$$

The nonfactorizable annihilation diagrams in Figs. 3(c) and 3(d) give

$$\mathcal{A}_{3(c,d)} = V^*_{ub}V_{ud}M^{LL}_{a\pi} - V^*_{tb}V_{td}(M'^{LL}_{a\pi} + M^{LR}_{a\pi}), \tag{A29}$$

with the amplitudes

$$\begin{aligned} M^{LL}_{a\pi} = {} & 32\pi C_F m_B^4/\sqrt{2N_c} \int dx_B dz dx_3 \int b_B db_B b_3 db_3 \phi_B(x_B,b_B) \\ & \times \{[(1-\eta)(\eta - (1+\eta)(x_B+z))\phi^A_\pi\phi_v + r\sqrt{\eta}(x_3(1-\eta)+\eta)(\phi^P_\pi + \phi^T_\pi)(\phi_s - \phi_t) \\ & - r\sqrt{\eta}(1-x_B-z)(\phi^P_\pi - \phi^T_\pi)(\phi_s+\phi_t) + 4r\sqrt{\eta}\phi^P_\pi\phi_s]C_1(t_{3c})E_{3cd}(t_{3c})h_{3c}(x_B,z,x_3,b_B,b_3) \\ & + [(1-\eta)(1-x_3(1-\eta) - \eta(1+x_B-z))\phi^A_\pi\phi_v - r\sqrt{\eta}(x_B-z)(\phi^P_\pi + \phi^T_\pi)(\phi_s-\phi_t) \\ & + r\sqrt{\eta}(1-\eta)(1-x_3)(\phi^P_\pi - \phi^T_\pi)(\phi_s+\phi_t)]C_1(t_{3d})E_{3cd}(t_{3d})h_{3d}(x_B,z,x_3,b_B,b_3)\}, \end{aligned} \tag{A30}$$

$$M'^{LL}_{a\pi} = M^{LL}_{a\pi}|_{C_1\to a_9}, \tag{A31}$$

$$\begin{aligned} M^{LR}_{a\pi} = {} & 32\pi C_F m_B^4/\sqrt{2N_c} \int dx_B dz dx_3 \int b_B db_B b_3 db_3 \phi_B(x_B,b_B) \\ & \times \{[\sqrt{\eta}(1-\eta)(2-x_B-z)\phi^A_\pi(\phi_s+\phi_t) - r(1+x_3)(\phi^P_\pi - \phi^T_\pi)\phi_v \\ & - r\eta[(1-x_B-z)(\phi^P_\pi + \phi^T_\pi) - x_3(\phi^P_\pi - \phi^T_\pi) + 2\phi^P_\pi]\phi_v]a_7(t_{3c})E_{3cd}(t_{3c})h_{3c}(x_B,z,x_3,b_B,b_3) \\ & - [r(1-\eta)(1-x_3)(\phi^P_\pi - \phi^T_\pi)\phi_v - \sqrt{\eta}(x_B-z)[r\sqrt{\eta}(\phi^P_\pi + \phi^T_\pi)\phi_v \\ & - (1-\eta)\phi^A_\pi(\phi_s+\phi_t)]]a_7(t_{3d})E_{3cd}(t_{3d})h_{3d}(x_B,z,x_3,b_B,b_3)\}. \end{aligned} \tag{A32}$$

Similarly, we derive from Figs. 4(a) and 4(b)

$$\mathcal{A}_{4(a,b)} = V^*_{ub}V_{ud}F^{LL}_{a\pi\pi} - V^*_{tb}V_{td}(F'^{LL}_{a\pi\pi} + F^{SP}_{a\pi\pi}), \tag{A33}$$

with the three-pion production amplitudes

$$F_{a\pi\pi}^{LL} = 8\pi C_F m_B^4 f_B \int dz dx_3 \int b db b_3 db_3 \times \{[2r\sqrt{\eta}\phi_\pi^P((2-z)\phi_s + z\phi_t) - (1-\eta)(1-z)\phi_\pi^A\phi_v]a_1(t_{4a})E_{4ab}(t_{4a})h_{4a}(z,x_3,b,b_3) + [2r\sqrt{\eta}[(1-x_3)(1-z)\phi_\pi^T - (1+x_3+(1-x_3)\eta)\phi_\pi^P]\phi_s + (x_3(1-\eta)+\eta)(1-\eta)\phi_\pi^A\phi_v]a_1(t_{4b})E_{4ab}(t_{4b})h_{4b}(z,x_3,b,b_3)\}, \tag{A34}$$

$$F_{a\pi\pi}^{\prime LL} = F_{a\pi\pi}^{LL}|_{a_1\to a_3}, \tag{A35}$$

$$F_{a\pi\pi}^{SP} = 16\pi C_F m_B^4 f_B \int dz dx_3 \int b db b_3 db_3 \{[\sqrt{\eta}(1-\eta)(1-z)\phi_\pi^A(\phi_s+\phi_t) - 2r(1+(1-z)\eta)\phi_\pi^P\phi_v] \times a_5(t_{4a})E_{4ab}(t_{4a})h_{4a}(z,x_3,b,b_3) + [2\sqrt{\eta}(1-\eta)\phi_\pi^A\phi_s - r(2\eta+x_3(1-\eta))\phi_\pi^P\phi_v + rx_3(1-\eta)\phi_\pi^T\phi_v] \times a_5(t_{4b})E_{4ab}(t_{4b})h_{4b}(z,x_3,b,b_3)\}, \tag{A36}$$

and from Figs. 4(c) and 4(d)

$$\mathcal{A}_{4(c,d)} = V_{ub}^* V_{ud} M_{a\pi\pi}^{LL} - V_{tb}^* V_{td}(M_{a\pi\pi}^{\prime LL} + M_{a\pi\pi}^{LR}), \tag{A37}$$

with the amplitudes

$$M_{a\pi\pi}^{LL} = 32\pi C_F m_B^4/\sqrt{2N_c} \int dx_B dz dx_3 \int b_B db_B b_3 db_3 \phi_B(x_B,b_B) \times \{[(\eta-1)[x_3(1-\eta)+x_B+\eta(1-z)]\phi_\pi^A\phi_v + r\sqrt{\eta}(x_3(1-\eta)+x_B+\eta)(\phi_\pi^P+\phi_\pi^T) \times (\phi_s-\phi_t) + r\sqrt{\eta}(1-z)(\phi_\pi^P-\phi_\pi^T)(\phi_s+\phi_t) + 2r\sqrt{\eta}(\phi_\pi^P\phi_s+\phi_\pi^T\phi_t)]C_1(t_{4c})E_{4cd}(t_{4c})h_{4c}(x_B,z,x_3,b_B,b_3) + [(1-\eta^2)(1-z)\phi_\pi^A\phi_v + r\sqrt{\eta}(x_B-x_3(1-\eta)-\eta)(\phi_\pi^P-\phi_\pi^T)(\phi_s+\phi_t) - r\sqrt{\eta}(1-z)(\phi_\pi^P+\phi_\pi^T)(\phi_s-\phi_t)]C_1(t_{4d})E_{4cd}(t_{4d})h_{4d}(x_B,z,x_3,b_B,b_3)\}, \tag{A38}$$

$$M_{a\pi\pi}^{\prime LL} = M_{a\pi\pi}^{LL}|_{C_1\to a_9}, \tag{A39}$$

$$M_{a\pi\pi}^{LR} = -32\pi C_F m_B^4/\sqrt{2N_c} \int dx_B dz dx_3 \int b_B db_B b_3 db_3 \phi_B(x_B,b_B) \times \{[\sqrt{\eta}(1-\eta)(1+z)\phi_\pi^A(\phi_s-\phi_t) + r(2-x_B-x_3(1-\eta))(\phi_\pi^P+\phi_\pi^T)\phi_v + r\eta(z\phi_\pi^P-(2+z)\phi_\pi^T)\phi_v]a_7(t_{4c})E_{4cd}(t_{4c})h_{4c}(x_B,z,x_3,b_B,b_3) + [\sqrt{\eta}(1-\eta)(1-z)\phi_\pi^A(\phi_s-\phi_t) + r(x_3(1-\eta)-x_B)(\phi_\pi^P+\phi_\pi^T)\phi_v + r\eta((2-z)\phi_\pi^P+z\phi_\pi^T)\phi_v]a_7(t_{4d})E_{4cd}(t_{4d})h_{4d}(x_B,z,x_3,b_B,b_3)\}. \tag{A40}$$

The threshold resummation factor $S_t(x)$ follows the parametrization in [30],

$$S_t(x) = \frac{2^{1+2c}\Gamma(3/2+c)}{\sqrt{\pi}\Gamma(1+c)}[x(1-x)]^c, \tag{A41}$$

in which the parameter is set to $c = 0.3$. The hard functions are written as

$$h_{1a}(x_B,z,b_B,b)=K_0(m_B\sqrt{x_Bz}b_B)[\theta(b_B-b)K_0(m_B\sqrt{z}b_B)I_0(m_B\sqrt{z}b)+(b\leftrightarrow b_B)]S_t(z),$$

$$h_{1b}(x_B,z,b_B,b)=K_0(m_B\sqrt{x_Bz}b_2)S_t(x_B)\times\begin{cases}\frac{i\pi}{2}[\theta(b-b_B)H_0^{(1)}(m_B\sqrt{\eta-x_B}b)J_0(m_B\sqrt{\eta-x_B}b_B)+(b\leftrightarrow b_B)], & x_B<\eta,\\ [\theta(b-b_B)K_0(m_B\sqrt{x_B-\eta}b)I_0(m_B\sqrt{x_B-\eta}b_B)+(b\leftrightarrow b_B)], & x_B\geq\eta,\end{cases}$$

$$h_{1c}(x_B,z,x_3,b_B,b_3)=[\theta(b_B-b_3)K_0(m_B\sqrt{x_Bz}b_B)I_0(m_B\sqrt{x_Bz}b_3)+(b_B\leftrightarrow b_3)]\times\begin{cases}\frac{i\pi}{2}H_0^{(1)}(m_B\sqrt{z[(1-\eta)(1-x_3)-x_B]}b_3), & (1-\eta)(1-x_3)>x_B,\\ K_0(m_B\sqrt{z[x_B-(1-\eta)(1-x_3)]}b_3), & (1-\eta)(1-x_3)\leq x_B,\end{cases}$$

$$h_{1d}(x_B,z,x_3,b_B,b_3)=[\theta(b_B-b_3)K_0(m_B\sqrt{x_Bz}b_B)I_0(m_B\sqrt{x_Bz}b_3)+(b_B\leftrightarrow b_3)]\times\begin{cases}\frac{i\pi}{2}H_0^{(1)}(m_B\sqrt{z[x_3(1-\eta)-x_B]}b_3), & x_3(1-\eta)>x_B,\\ K_0(m_B\sqrt{z[x_B-x_3(1-\eta)]}b_3), & x_3(1-\eta)\leq x_B,\end{cases}$$

$$h_{2a}(x_B,x_3,b_B,b_3)=K_0(m_B\sqrt{x_Bx_3(1-\eta)}b_B)[\theta(b_B-b_3)K_0(m_B\sqrt{x_3(1-\eta)}b_B)\times I_0(m_B\sqrt{x_3(1-\eta)}b_3)+(b_3\leftrightarrow b_B)]S_t(x_3),$$

$$h_{2b}(x_B,x_3,b_B,b_3)=h_{2a}(x_3,x_B,b_3,b_B),$$

$$h_{2c}(x_B,z,x_3,b_B,b)=[\theta(b_B-b)K_0(m_B\sqrt{x_Bx_3(1-\eta)}b_B)I_0(m_B\sqrt{x_Bx_3(1-\eta)}b)+(b_B\leftrightarrow b)]\begin{cases}\frac{i\pi}{2}H_0^{(1)}(m_B\sqrt{(1-x_B-z)[x_3(1-\eta)+\eta]}b), & x_B+z<1,\\ K_0(m_B\sqrt{(x_B+z-1)[x_3(1-\eta)+\eta]}b), & x_B+z\geq 1,\end{cases}$$

$$h_{2d}(x_B,z,x_3,b_B,b)=[\theta(b_B-b)K_0(m_B\sqrt{x_Bx_3(1-\eta)}b_B)I_0(m_B\sqrt{x_Bx_3(1-\eta)}b)+(b_B\leftrightarrow b)]\begin{cases}\frac{i\pi}{2}H_0^{(1)}(m_B\sqrt{x_3(z-x_B)(1-\eta)}b), & x_B<z,\\ K_0(m_B\sqrt{x_3(x_B-z)(1-\eta)}b), & x_B\geq z,\end{cases}$$

$$h_{3a}(z,x_3,b,b_3)=\left(\frac{i\pi}{2}\right)^2H_0^{(1)}(m_B\sqrt{(1-x_3)z(1-\eta)}b)S_t(x_3)\times[\theta(b-b_3)H_0^{(1)}(m_B\sqrt{1-x_3(1-\eta)}b)J_0(m_B\sqrt{1-x_3(1-\eta)}b_3)+(b\leftrightarrow b_3)],$$

$$h_{3b}(z,x_3,b,b_3)=\left(\frac{i\pi}{2}\right)^2H_0^{(1)}(m_B\sqrt{(1-x_3)z(1-\eta)}b_3)S_t(z)\times[\theta(b-b_3)H_0^{(1)}(m_B\sqrt{z(1-\eta)}b)J_0(m_B\sqrt{z(1-\eta)}b_3)+(b\leftrightarrow b_3)],$$

$$h_{3c}(x_B,z,x_3,b_B,b_3)=\frac{i\pi}{2}K_0(m_B\sqrt{1-x_3(1-x_B-z)(1-\eta)+(x_B+z-1)\eta}b_B)\times[\theta(b_B-b_3)H_0^{(1)}(m_B\sqrt{(1-x_3)z(1-\eta)}b_B)J_0(m_B\sqrt{(1-x_3)z(1-\eta)}b_3)+(b_B\leftrightarrow b_3)],$$

$$h_{3d}(x_B,z,x_3,b_B,b_3)=\frac{i\pi}{2}[\theta(b_B-b_3)H_0^{(1)}(m_B\sqrt{(1-x_3)z(1-\eta)}b_B)J_0(m_B\sqrt{(1-x_3)z(1-\eta)}b_3)+(b_B\leftrightarrow b_3)]\times\begin{cases}\frac{i\pi}{2}H_0^{(1)}(m_B\sqrt{(1-x_3)(z-x_B)(1-\eta)}b_B), & x_B<z,\\ K_0(m_B\sqrt{(1-x_3)(x_B-z)(1-\eta)}b_B), & x_B\geq z,\end{cases}$$

$$h_{4a}(z,x_3,b,b_3)=\left(\frac{i\pi}{2}\right)^2H_0^{(1)}(m_B\sqrt{(1-z)(\eta+x_3(1-\eta))}b_3)S_t(z)\times[\theta(b-b_3)H_0^{(1)}(m_B\sqrt{1-z}b)J_0(m_B\sqrt{1-z}b_3)+(b\leftrightarrow b_3)],$$

$$h_{4b}(z,x_3,b,b_3)=\left(\frac{i\pi}{2}\right)^2H_0^{(1)}(m_B\sqrt{(1-z)(\eta+x_3(1-\eta))}b)S_t(x_3)\times[\theta(b-b_3)H_0^{(1)}(m_B\sqrt{\eta+x_3(1-\eta)}b)J_0(m_B\sqrt{\eta+x_3(1-\eta)}b_3)+(b\leftrightarrow b_3)],$$

$$
\begin{aligned}
h_{4c}(x_B, z, x_3, b_B, b_3) &= \frac{i\pi}{2} K_0(m_B\sqrt{1-z((1-x_3)(1-\eta)-x_B)}b_B) \\
&\quad \times [\theta(b_B-b_3)H_0^{(1)}(m_B\sqrt{(1-z)(\eta+x_3(1-\eta))}b_B)J_0(m_B\sqrt{(1-z)(\eta+x_3(1-\eta))}b_3) \\
&\quad + (b_B\leftrightarrow b_3)], \\
h_{4d}(x_B, z, x_3, b, b_3) &= \frac{i\pi}{2}[\theta(b_B-b_3)H_0^{(1)}(m_B\sqrt{(1-z)(\eta+x_3(1-\eta))}b_B) \\
&\quad \times J_0(m_B\sqrt{(1-z)(\eta+x_3(1-\eta))}b_3) + (b_B\leftrightarrow b_3)] \\
&\quad \times \begin{cases} \frac{i\pi}{2}H_0^{(1)}(m_B\sqrt{(1-z)(\eta+x_3(1-\eta)-x_B)}b_B), & x_B < \eta + x_3(1-\eta), \\ K_0(m_B\sqrt{(1-z)(x_B-\eta-x_3(1-\eta))}b_B), & x_B \geq \eta+x_3(1-\eta), \end{cases}
\end{aligned} \tag{4.40}
$$

with the Hankel function $H_0^{(1)}(x) = J_0(x) + iY_0(x)$.

The evolution factors in the above factorization formulas are given by

$$
\begin{aligned}
&E_{1ab}(t) = \alpha_s(t)\exp[-S_B(t) - S_{Ms}(t)], \qquad E_{1cd}(t) = \alpha_s(t)\exp[-S_B(t) - S_{Ms}(t) - S_\pi]|_{b=b_B}, \\
&E_{2ab}(t) = \alpha_s(t)\exp[-S_B(t) - S_\pi(t)], \qquad E_{2cd}(t) = \alpha_s(t)\exp[-S_B(t) - S_{Ms}(t) - S_\pi]|_{b_3=b_B}, \\
&E_{3ab}(t) = \alpha_s(t)\exp[-S_{Ms} - S_\pi(t)], \qquad E_{3cd}(t) = \alpha_s(t)\exp[-S_B(t) - S_{Ms}(t) - S_\pi]|_{b_3=b}, \\
&E_{4ab}(t) = E_{3ab}(t), \qquad E_{4cd}(t) = E_{3cd}(t),
\end{aligned} \tag{A43}
$$

in which the Sudakov exponents are defined as

$$
\begin{aligned}
S_B &= s\left(x_B\frac{m_B}{\sqrt{2}}, b_B\right) + \frac{5}{3}\int_{1/b_B}^{t}\frac{d\bar{\mu}}{\bar{\mu}}\gamma_q(\alpha_s(\bar{\mu})), \qquad S_{Ms} = s\left(z\frac{m_B}{\sqrt{2}}, b\right) + s\left((1-z)\frac{m_B}{\sqrt{2}}, b\right) + 2\int_{1/b}^{t}\frac{d\bar{\mu}}{\bar{\mu}}\gamma_q(\alpha_s(\bar{\mu})), \\
S_\pi &= s\left(x_3\frac{m_B}{\sqrt{2}}, b_3\right) + s\left((1-x_3)\frac{m_B}{\sqrt{2}}, b_3\right) + 2\int_{1/b_3}^{t}\frac{d\bar{\mu}}{\bar{\mu}}\gamma_q(\alpha_s(\bar{\mu})),
\end{aligned} \tag{A44}
$$

with the quark anomalous dimension $\gamma_q = -\alpha_s/\pi$. The explicit expressions of the functions $s(Q, b)$ can be found, for example, in Appendix A of Ref. [25]. The involved hard scales are chosen in the PQCD approach as

$$
\begin{aligned}
&t_{1a} = \max\{m_B\sqrt{z}, 1/b_B, 1/b\}, \qquad t_{1b} = \max\{m_B\sqrt{|x_B-\eta|}, 1/b_B, 1/b\}, \\
&t_{1c} = \max\{m_B\sqrt{x_B z}, m_B\sqrt{z|(1-\eta)(1-x_3)-x_B|}, 1/b_B, 1/b_3,\}, \\
&t_{1d} = \max\{m_B\sqrt{x_B z}, m_B\sqrt{z|x_B-x_3(1-\eta)|}, 1/b_B, 1/b_3\}, \qquad t_{2a} = \max\{m_B\sqrt{x_3(1-\eta)}, 1/b_B, 1/b_3\}, \\
&t_{2b} = \max\{m_B\sqrt{x_B(1-\eta)}, 1/b_B, 1/b_3\}, \qquad t_{2c} = \max\{m_B\sqrt{x_B x_3(1-\eta)}, m_B\sqrt{|1-x_B-z|[x_3(1-\eta)+\eta]}, 1/b_B, 1/b,\}, \\
&t_{2d} = \max\{m_B\sqrt{x_B x_3(1-\eta)}, m_B\sqrt{|x_B-z|x_3(1-\eta)}, 1/b_B, 1/b\}, \qquad t_{3a} = \max\{m_B\sqrt{1-x_3(1-\eta)}, 1/b, 1/b_3\}, \\
&t_{3b} = \max\{m_B\sqrt{z(1-\eta)}, 1/b, 1/b_3\}, \\
&t_{3c} = \max\{m_B\sqrt{(1-x_3)z(1-\eta)}, m_B\sqrt{1-x_3(1-x_B-z)(1-\eta)+(x_B+z-1)\eta}, 1/b_B, 1/b_3,\}, \\
&t_{3d} = \max\{m_B\sqrt{(1-x_3)z(1-\eta)}, m_B\sqrt{|x_B-z|(1-x_3)(1-\eta)}, 1/b_B, 1/b_3\}, \\
&t_{4a} = \max\{m_B\sqrt{1-z}, 1/b, 1/b_3\}, \qquad t_{4b} = \max\{m_B\sqrt{\eta+x_3(1-\eta)}, 1/b, 1/b_3\}, \\
&t_{4c} = \max\{m_B\sqrt{(1-z)(\eta+x_3(1-\eta))}, m_B\sqrt{1-z((1-x_3)(1-\eta)-x_B)}, 1/b_B, 1/b_3,\}, \\
&t_{4d} = \max\{m_B\sqrt{(1-z)(\eta+x_3(1-\eta))}, m_B\sqrt{(1-z)|x_B-\eta-x_3(1-\eta)|}, 1/b_B, 1/b_3\}.
\end{aligned} \tag{A45}
$$

[1] C. H. Chen and H.-n. Li, Phys. Lett. B **561**, 258 (2003).
[2] H. Y. Cheng and K. C. Yang, Phys. Rev. D **66**, 054015 (2002);H.-Y. Cheng, C.-K. Chua, and A. Soni, Phys. Rev. D **76**, 094006 (2007).
[3] S. Fajfer, T. N. Pham, and A. Prapotnik, Phys. Rev. D **70**, 034033 (2004).
[4] B. Bhattacharya, M. Imbeault, and D. London, Phys. Lett. B **728**, 206 (2014); N. R.-L. Lorier, M. Imbeault, and D. London, Phys. Rev. D **84**, 034040 (2011);M. Imbeault, N. R.-L. Lorier, and D. London, Phys. Rev. D **84**, 034041 (2011);N. R.-L Lorier and D. London, Phys. Rev. D **85**, 016010 (2012).
[5] R. Aaij *et al.* (LHCb Collaboration), Phys. Rev. Lett. **111**, 101801 (2013).
[6] R. Aaij *et al.* (LHCb Collaboration), Phys. Rev. Lett. **112**, 011801 (2014).
[7] I. Nasteva (LHCb Collaboration), arXiv:1308.0740;J. M. de Miranda (LHCb Collaboration), arXiv:1301.0283.
[8] Z. H. Zhang, X. H. Guo, and Y. D. Yang, Phys. Rev. D **87**, 076007 (2013).
[9] B. Bhattacharya, M. Gronau, and J. L. Rosner, Phys. Lett. B **726**, 337 (2013).
[10] D. Xu, G. N. Li, and X. G. He, Int. J. Mod. Phys. A **29**, 1450011 (2014);Phys. Lett. B **728**, 579 (2014).
[11] H. Y. Cheng and C. K. Chua, Phys. Rev. D **88**, 114014 (2013);arXiv:1401.5514 [Phys. Rev. D (to be published)]; Y. Li, arXiv:1401.5948.
[12] C. L. Y. Lee, M. Lu, and M. B. Wise, Phys. Rev. D **46**, 5040 (1992).
[13] Y. Y. Keum, H.-n. Li, and A. I. Sanda, Phys. Lett. B **504**, 6 (2001);Y. Y. Keum, H.-n. Li, and A. I. SandaPhys. Rev. D **63**, 054008 (2001).
[14] C. D. Lu, K. Ukai, and M. Z. Yang, Phys. Rev. D **63**, 074009 (2001).
[15] D. Muller, D. Robaschik, B. Geyer, F.-M. Dittes, and J. Hořejši, Fortschr. Phys. **42**, 101 (1994);M. Diehl, T. Gousset, B. Pire, and O. Teryaev, Phys. Rev. Lett. **81**, 1782 (1998);M. V. Polyakov, Nucl. Phys. **B555**, 231 (1999).
[16] M. Diehl, T. Gousset, and B. Pire, Phys. Rev. D **62**, 073014 (2000).
[17] J. Beringer *et al.* (Particle Data Group), Phys. Rev. D **86**, 010001 (2012).
[18] M. R. Whalley, J. Phys. G **29**, A1 (2003);J. Milana, S. Nussinov, and M. G. Olsson, Phys. Rev. Lett. **71**, 2533 (1993);T. K. Pedlar *et al.*, Phys. Rev. Lett. **95**, 261803 (2005).
[19] H. C. Hu and H.-n. Li, Phys. Lett. B **718**, 1351 (2013).
[20] S. D. Protopopescu, Phys. Rev. D **7**, 1279 (1973).
[21] P. Estabrooks and A. D. Martin, Nucl. Phys. **B79**, 301 (1974).
[22] J. H. Kuhn and A. Santamaria, Z. Phys. C **48**, 445 (1990).
[23] P. Ball and R. Zwicky, Phys. Rev. D **71**, 014015 (2005); P. Ball, V. M. Braun, and A. Lenz, J. High Energy Phys. 05 (2006) 004.
[24] P. Colangelo, F. De Fazio, P. Santorelli, and E. Scrimieri, Phys. Rev. D **53**, 3672 (1996);A. Khodjamirian, T. Mannel, and N. Offen, Phys. Rev. D **75**, 054013 (2007); M. A. Ivanov, J. G. Korner, S. G. Kovalenko, and C. D. Roberts, Phys. Rev. D **76**, 034018 (2007);D. Ebert, R. N. Faustov, and V. O. Galkin, Phys. Rev. D **75**, 074008 (2007);X. G. Wu and T. Huang, Phys. Rev. D **79**, 034013 (2009);W. F. Wang and Z. J. Xiao, Phys. Rev. D **86**, 114025 (2012).
[25] A. Ali, G. Kramer, Y. Li, C. D. Lü, Y. L. Shen, W. Wang, and Y. M. Wang, Phys. Rev. D **76**, 074018 (2007).
[26] H.-n. Li and S. Mishima, Phys. Rev. D **74**, 094020 (2006).
[27] C. H. Chen and H.-n. Li, Phys. Rev. D **70**, 054006 (2004).
[28] L. Li, B. S. Zou, and G. L. Li, Phys. Rev. D **67**, 034025 (2003).
[29] M. Doring, U. G. Meisner, and W. Wang, J. High Energy Phys. 10 (2013) 011;U. G. Meisner and W. Wang, Phys. Lett. B **730**, 336 (2014).
[30] T. Kurimoto, H.-n. Li, and A. I. Sanda, Phys. Rev. D **65**, 014007 (2001).